Raman scattering studies of the impurity-induced ferroelectric phase transition in $KTaO_3$:Li

R. L. Prater and L. L. Chase
Physics Department, Indiana University, Bloomington, Indiana 47405

L. A. Boatner
Solid State Division, Oak Ridge National Laboratory, Oak Ridge, Tennessee 37830

(Received 12 January 1981)

Raman scattering and optical depolarization measurements have been employed in investigations of the phase transition induced by the substitution of lithium for potassium in $KTaO_3$ to form $K_{1-x}Li_xTaO_3$. Lithium concentrations as high as 5.4 mol% were studied. At low concentrations, $x \leq 0.004$, the intensities of the disorder-induced scattering features observed for pure $KTaO_3$ increase as the Li fraction increases. A low-frequency feature, which was previously associated with a Li resonance mode, appears to be scattering from the coupled TA and TO branches due to disorder introduced by the lithium. For $x \gtrsim 0.01$, a clearly defined step in the optical depolarization is observed at a temperature T_c which increases rapidly with lithium concentration and reaches a value of $T_c = 70$ K at $x = 0.054$. The dependence on the polarization direction of the incident light indicates that a tetragonal or orthorhombic low-temperature phase is formed with $\langle 100 \rangle$ symmetry axes. New Raman-active phonons are observed near and below T_c. The anisotropy of the energy of the extraordinary phonon expected from polar modes is not observed in the unpoled samples. Poling can be accomplished by cooling the crystals through T_c with an applied electric field, after which the polar character of these phonons is observed. The lack of anisotropy in unpoled samples is the result of the presence of ferroelectric domains with diameters smaller than optical wavelengths. Additionally, the depolarization measurements imply domain sizes of at least a few thousand Å. These results clearly disagree with the previous claims that $K_{1-x}Li_xTaO_3$ is not ferroelectric for $x < 0.24$ and that the Li centers form a polar glass at low temperatures. Finally, the presence of the lithium impurities stiffens the TO branch at the zone center, and the ferroelectric phase results from an order-disorder transition of the off-center lithium ions.

I. INTRODUCTION

A relatively recent review of the dynamics of phase transitions by Halperin and Varma[1] has served to stimulate increased interest in the related topic of the effects of impurities on phase transitions. In particular, a number of investigations of ferroelectric phase transitions induced by the addition of impurities to incipient ferroelectric crystals (e.g., $KTaO_3$) have recently been carried out.[2–7] In one of these investigations,[2] the present authors have employed the techniques of Raman scattering and optical depolarization to study the properties of a ferroelectric phase transition induced by the addition of niobium impurities to $KTaO_3$. In the work reported here, similar investigations of $K_{1-x}Li_xTaO_3$ have addressed questions related to the types of impurities that are capable of inducing a phase transition, the responsible mechanisms, and the characterization of different types of phase transitions. The present results for $K_{1-x}Li_xTaO_3$ reveal behavior that is quite different from that found previously for $KTa_{1-x}Nb_xO_3$.

Any study of impurity effects naturally proceeds from an understanding of the behavior of the pure material. The results of numerous prior investigations of pure $KTaO_3$ were briefly summarized in Ref. 2 (which also included a discussion of new evidence for disorder-induced effects in this substance), and this background material will not be repeated here. It is important, however, to be aware of the manifestations of the disorder-induced effects in the Raman spectra that were presented in Ref. 2 as a basis for understanding the effects of lithium impurities on the Raman spectra presented in the current work.

The $K_{1-x}Li_xTaO_3$ system was first investigated by Yacoby and Linz,[3] and Yacoby and Yust[4] have used Raman scattering in observing the low-frequency spectra of mixed crystals with either lithium or sodium impurities in concentrations greater than 5 mol%. These workers identified what they believed to be impurity vibrational modes which softened in frequency as the temperature was decreased until a ferroelectric

phase transition occurred at about 80 K in $K_{0.95}Li_{0.05}TaO_3$. In a later paper, Yacoby *et al.*[5] studied the same features as a function of pressure, and concluded that Li (or Na) ions occupy substitutional potassium sites in the $KTaO_3$ lattice but are somewhat displaced from the symmetrical positions of these sites. As will be shown here, the conclusions that lithium impurities occupy off-center positions in the lattice, and that the resultant dipoles are responsible for a phase transition, both seem valid, although the interpretation of the Raman spectra and the nature of the phase transition are quite different from that given by Yacoby *et al.*

Recent work by Höchli *et al.*[6,7] indicated that $KTaO_3$:Li does not become ferroelectric at low temperatures in samples with lithium concentrations up to 24 mol%. The evidence they presented consisted of a failure to observe a spontaneous polarization at any temperature and the absence of a step in the elastic compliance similar to the step associated with the phase change in $KTaO_3$:Nb. They attempted to explain the apparent conflict between the existence of polarized lithium defects and the absence of bulk ferroelectric properties by postulating what was termed a ferroelectric "spin-glass" structure that was characterized by domain sizes on the order of 10 to 100 lattice spacings.

The present studies concentrate on the Raman scattering spectral features and their polarization at low frequencies (less than 200 cm^{-1}). The spectra have been studied as a function of temperature and applied uniaxial strain for several low concentrations of lithium in the range between 0.2 and 5.4 mol%. The scattering for different experimental geometries in otherwise identical samples, both poled and unpoled, was also compared. In addition, measurements of the depolarization of light as it passes through the samples were made at various temperatures. These experiments indicate that a phase transition does indeed occur, at least for lithium concentrations $\gtrsim 1$ mol%, and the results are consistent with a tetragonally distorted, low-temperature ferroelectric phase.

II. EXPERIMENTAL TECHNIQUES

The apparatus and procedures employed in the general Raman scattering and depolarization measurements were identical to those described in Ref. 2. A special sample holder was used, however, in studies of the Raman spectrum as a function of applied uniaxial stress. These experiments were only performed for samples having a transition temperature below ~ 70 K. A liquid-nitrogen bath in contact with the sample chamber, which contained a nitrogen gas atmosphere, maintained the sample temperature at 77 K. The samples, which were cut to dimensions of $\sim 1.5 \times 3 \times 5$ mm^3 and optically polished, were placed between two stainless-steel pistons which moved freely inside a stainless-steel cylinder. The lower piston contacted a piezoelectric transducer at the bottom of the cylinder, which was used to measure the force applied to the sample. A stainless-steel tube transmitted the force from a pneumatic cylinder at the top of the cryostat to the upper piston, and small pieces of computer card coated with silicone grease were placed between the sample and each piston to reduce any inhomogeneity in the applied stress. Further details of the stress apparatus can be found elsewhere.[8]

The poling experiments were done by cooling the sample from 77 K while applying a constant bias voltage across the sample. The slab shaped sample was coated on the two opposing broad faces with a conducting silver paint with a small area left open on one face. The copper sample holder formed the ground connection and thermal sink for the sample. The opposite electrode was a thin copper plate with a 1-mm hole through the center to allow a laser beam to be incident parallel to the direction of the poling electric field. The maximum potential that could be maintained during the cooling with the 5.4 mol% Li sample in 1 atm of He gas was 250 V across a sample 1.6-mm thick. Thus, a bias field of 1.6 kV/cm was sufficient to pole the 5.4 mol% Li sample. In agreement with the results of Höchli *et al.*,[7] a sample cooled from room temperature without a bias field could not be poled at 4.2 K with fields that could be applied without breakdown.

The $K_{1-x}Li_xTaO_3$ single-crystal samples were grown from a mixture of K_2CO_3, Ta_2O_5, and varying amounts of Li_2CO_3 which was placed in a platinum crucible. The data are reported by labeling the samples with the molar ratio of Li_2CO_3 to K_2CO_3 used in the initial mixture, even though the mixture includes an excess of K_2CO_3 which forms a flux during crystal growth. Further details of the process can be found elsewhere.[9] When viewed between crossed polarizers, these crystals frequently have areas in which the polarization is rotated. These areas seem somewhat elongated and the longer axes are oriented parallel to $\langle 110 \rangle$ crystallographic directions. They vary widely in number and size from one sample to another and are presumably the result of internal strains.

III. EXPERIMENTAL RESULTS

A. Changes in the Raman spectra due to lithium impurities

A number of samples containing small amounts of lithium have been studied in order to determine how the features of the Raman spectra of pure $KTaO_3$ change as a function of increasing lithium concentra-

tion. In Fig. 1 the Raman spectrum at $T=4.2$ K of a pure $KTaO_3$ sample is compared with the spectra of samples containing 0.2 and 0.4 mol% Li. The features at 15, ~30, and 197 cm^{-1} were found to increase in intensity roughly in proportion to the lithium concentration. Two of these features can be attributed to disorder-induced scattering peaks from the TA branch, denoted by A, and from the TO_2 branch.[2] The feature labeled B is a new lithium-induced peak superimposed on a broad shoulder extending from 20 cm^{-1} up to the 2TA peak. This shoulder was identified in Ref. 2 as disorder-induced scattering from the soft TO_1 branch.

Yacoby and Yust[4] concluded that the A peak in $KTaO_3$:Li was an impurity resonance mode due to lithium. The reasoning for this conclusion relies mainly on an analogy between the A peak in $KTaO_3$:Li and a similar peak at much higher energies in $KTaO_3$ containing sodium. They reasoned that the different energies of the peaks associated with each impurity preclude the alternate possibility that these features are due to impurity-induced scattering from host lattice modes. Following this work, several studies by Höchli *et al.*[6,10] showed that the behavior of the $KTaO_3$:Na system differs from that of $KTaO_3$:Li in several important ways which will be discussed further in the conclusions of this paper. With the added understanding of the importance of disorder-induced scattering in the Raman spectra of pure $KTaO_3$, the nature of the A peak in $KTaO_3$:Li becomes clear; the presence of lithium impurities enhances the disorder-induced scattering[2] from the TA branch along ⟨100⟩ directions, where coupling to the TO_1 branch produces a "kink" in the TA dispersion.[11] While these data suggest that the off-center Li ions are an effective source of disorder which breaks the usual $k \cong 0$ Raman selection rule, it should be noted that the disorder-induced scattering is seen even in samples grown with ultrapure starting materials using great care to avoid any remnant lithium contamination. In only one nominally pure sample have any of these features been clearly reduced in intensity; this was the only sample that was examined in which no evidence for the presence of OH^- was found in the infrared absorption spectrum.[12] Accordingly, it is evident that residual lithium impurities do not represent the sole source of disorder-induced scattering in nominally pure $KTaO_3$.

In samples with lithium concentrations greater than about 1% the induced phase transition prevents a meaningful comparison of the spectra with the spectrum of the pure material at 4.2 K. A comparison of samples containing 1.4, 2.2, and 5.4 mol% Li at 77 K, however, is shown in Fig. 2. Again, it is clear that the intensities of peak A, the B line, and the TO_2 branch increase with increased lithium concentration in the high-temperature, paraelectric phase. It is probably not valid to attempt to quantitatively analyze the relationship between the intensities of these features and the lithium concentration in Fig. 2 for several reasons. First, there is some uncertainty in the actual lithium concentration in the lattice; i.e., the labels indicate the ratio of lithium to potassium atoms in the growth mixture. Second, a feature must be found that remains unaffected by the impurity so that it can be used as a calibration for determining

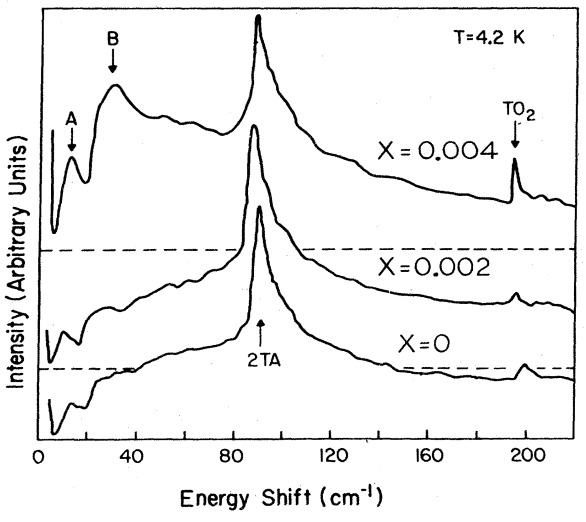

FIG. 1. Raman spectra of $K_{1-x}Li_xTaO_3$ with $x=0.002$ and 0.004, compared to the spectrum of pure $KTaO_3$ at $T=4.2$ K. Polarizations included are $Y(ZZ)X$ and $Y(ZY)X$, where X, Y, and Z are pseudocubic axes.

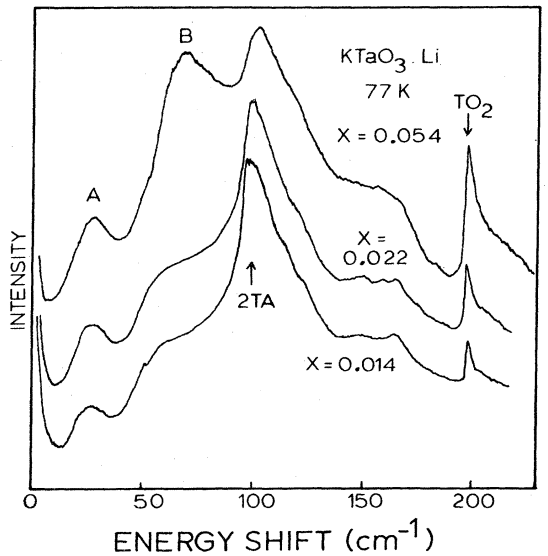

FIG. 2. Raman spectra of $K_{1-x}Li_xTaO_3$ with $x=0.014$, 0.022, and 0.054 at $T=77$ K. Polarizations included are the same as in Fig. 1.

the intensity of the other features. The 2TA peak near 100 cm^{-1} was generally used for this purpose, but it is possible that this peak could be broadened slightly or otherwise affected by the presence of the impurity. Third, and perhaps most importantly, the phase transition occurs at a different temperature in each sample. At 77 K, the sample containing 5.4 mol% Li is much closer to the transition temperature, and the onset of changes which occur near the transition would invalidate comparisons with other samples. This problem demonstrates the need for interpreting the spectra with some knowledge of the transition temperature.

B. Measurements of phase transition temperatures

Two methods were used to determine approximate temperatures for the phase transition. One approach was to measure the depolarization of light as it passed through the sample. In Fig. 3, the depolarization ratio

$$R = \frac{I_{\parallel} - I_{\perp}}{I_{\parallel} + I_{\perp}}$$

is plotted as a function of temperature for several samples with different Li concentrations. The incident light is polarized along a ⟨110⟩ axis. It is clear that for higher Li concentrations there is a true phase change. Above a certain temperature there is no depolarization, and below that temperature the depolarization ratio decreases rapidly. If the low-temperature state is truly glassy, as suggested by Höchli *et al.*,[7] the light would travel through a medium with an averaged, isotropic index of refraction and there would be little depolarization. The fact that the light is depolarized indicates that there are sizable regions of the sample with anisotropic refractive properties. The implications of these data will be discussed more fully in Sec. IV B.

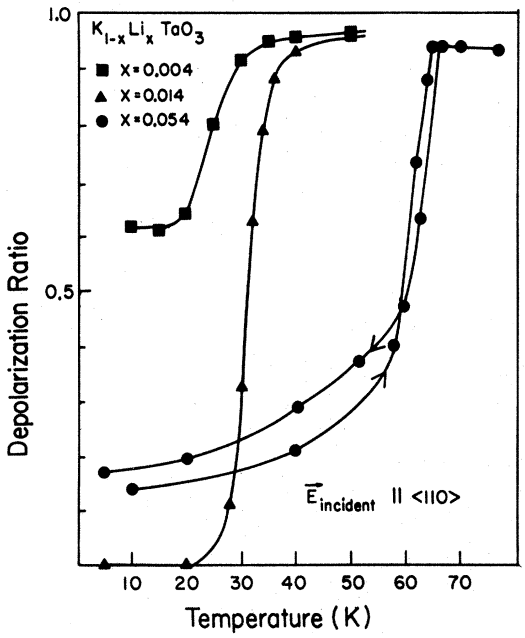

FIG. 3. Depolarization of light polarized along a ⟨110⟩ crystal axis by $K_{1-x}Li_xTaO_3$ samples with $x = 0.004$, 0.014, and 0.054.

The depolarization data for samples with lithium concentrations ≤ 1 mol% show that the light is not completely depolarized. These samples did not behave like birefringent crystals when the analyzer was rotated; hence, the effect is best described as a partial depolarization. Two distinct mechanisms might cause such a partial depolarization. First, the sample may have isotropic refractive indices throughout most of the bulk with a few isolated, noninteracting regions with anisotropic refractive indices so that the cumulative effect is a partial depolarization of the total beam. Alternately, an incomplete depolarization could result if a large number of domains individually only slightly alter the polarization.

Another feature of the data presented in Fig. 3 is that the curves do not give an indication of a very sharp transition with a well-defined T_c. At best, T_c can be determined within a 5-K range by noting when the depolarization effects begin as the temperature is decreased. Thus, the implication is that either the transitions are broadened or the detailed nature of the onset of depolarization accompanying a phase transition is not well understood. Possible inhomogeneities in either Li concentration or internal strain complicate the situation even more.

The depolarization measurements also indicate the symmetry of the low-temperature phase in the $K_{1-x}Li_xTaO_3$ system. If the incoming beam is polarized parallel to a ⟨100⟩ direction, the light is only slightly depolarized by the sample, and even then the depolarization is primarily only in the immediate vicinity of the transition temperature. If the incoming beam is polarized parallel to a ⟨110⟩ direction, the light is almost completely depolarized. This indicates that the principal axes of the index of refraction tensor in the low-symmetry phase are oriented along ⟨100⟩ axes rather than ⟨110⟩ or ⟨111⟩ directions. Thus, the lithium-induced low-temperature phase must either have tetragonal or orthorhombic symmetry in contrast to the rhombohedral phase of $KTa_{1-x}Nb_xO_3$ for $x < 0.06$.[13]

The second method which was used to determine the temperature of the phase transition is to monitor the changes in the Raman spectra as a function of temperature. The temperature dependence of the spectrum of a sample containing 5.4 mol% Li is shown in Fig. 4. As the temperature decreases from 250 K, the intensity of the scattering from the TA

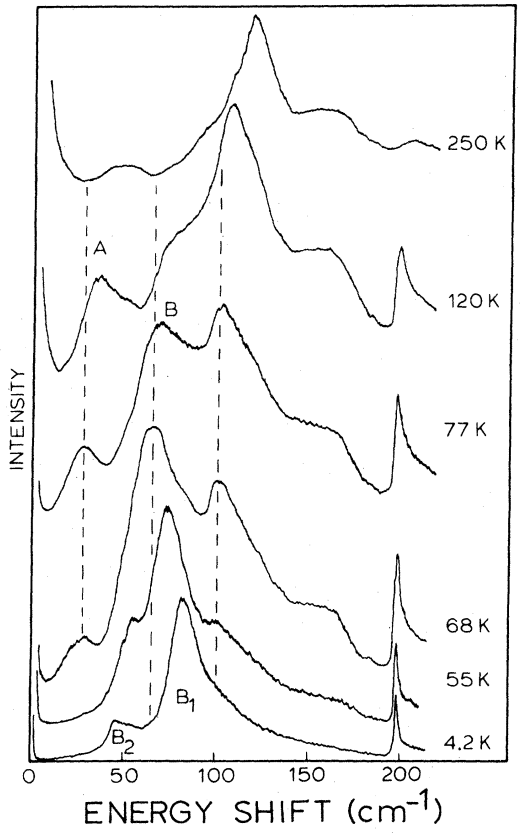

FIG. 4. Temperature dependence of the Raman spectrum of $KTaO_3$ containing 5.4 mol% Li. Polarizations included are the same as in Fig. 1.

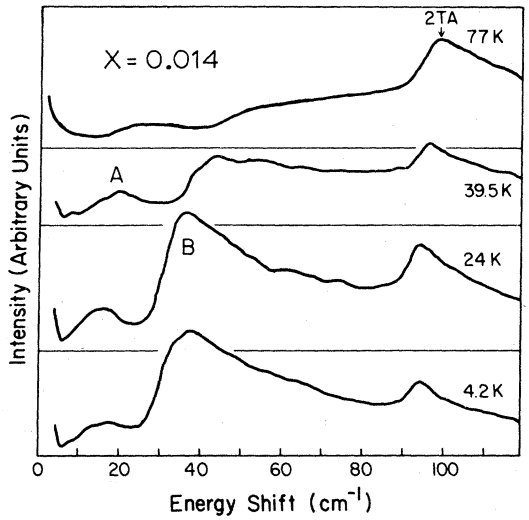

FIG. 5. Temperature dependence of the Raman spectrum of $KTaO_3$ containing 1.4 mol% Li. Polarizations included are the same as in Fig. 1.

branch (peak A, near 50 cm^{-1} at 250 K) increases and then disappears below the phase transition. It softens, but only to a minimum energy near 25 cm^{-1} where the peak can no longer be detected. The intensity of the scattering from the TO_2 branch at 197 cm^{-1} increases as the temperature approaches T_c and then remains almost constant relative to the intensity of the 2TA peak in the temperature range below the transition. As the temperature is decreased near 77 K, the B peak grows in intensity until it dominates the TO_1 branch shoulder.[2] This peak gradually splits into two components labeled B_1 and B_2 below the 68-K transition. The temperature at which this splitting begins provides an additional measurement of T_c. There is some uncertainty in determining an exact value for T_c with either of the methods described above, but both methods give consistent T_c values in the present case. A $KTaO_3$ sample containing 2.2 mol% Li definitely shows a phase transition at some temperature in the neighborhood of 40 to 45 K, but this transition is not as well defined in either the depolarization data or the Raman spectra as it is in the case of the sample containing 5.4 mol% Li. The splitting of the new, Raman-active modes below the transition is not fully resolved for the sample with 2.2 mol% Li even when the temperature is lowered to 4.2 K. Similar features are also apparent from the data shown in Fig. 5 for a sample containing 1.4 mol% Li. In this case, the depolarization in Fig. 3 is essentially complete below 20 K, but the Raman spectra only show an increase in the intensity of the shoulder to form a peak and a broadening of the shoulder when the sample temperature is 4.2 K.

C. Temperature dependence of the spectral features

The temperature dependence of the energies of several features in the Raman spectra for various lithium concentrations is plotted in Fig. 6. The data from the sample containing 5.4 mol% Li indicate that the two vibrational modes observed below the transition temperature are the split components of a single mode found in the high-temperature, cubic phase. This splitting occurs near 70 K, a temperature which is near the T_c determined from the depolarization studies. For the sample grown with 2.2 mol% Li, Fig. 6 shows that there is no resolved splitting, but there is an increasing width of the peak as the temperature is lowered below T_c.

No features were found in these spectra which could be associated with a soft mode either below the transition temperature or in the disorder-induced scattering observed above the transition. The data in Fig. 6 indicate that the disorder-induced scattering from the TA branch softened, but the peak was never detected below about 12 cm^{-1}. In fact, when T_c is near 68 K, the minimum energy of this peak is 25 cm^{-1}. The other possibility for a soft-mode feature is

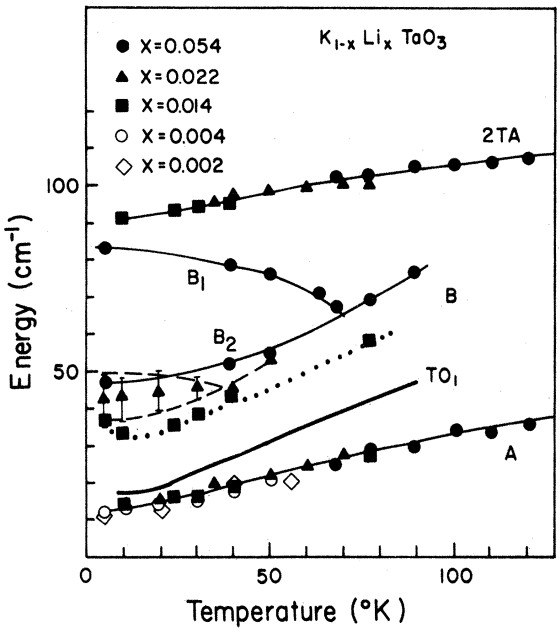

FIG. 6. Energies of the low-frequency spectral features vs temperature for $KTaO_3$:Li. The vertical lines associated with the triangle near 45 cm^{-1} indicate the width of this peak in this particular sample. The line labeled "TO_1" is the energy of the TO phonon in pure $KTaO_3$.

represented by the disorder-induced scattering from the TO_1 branch. As expected,[2] this scattering was always seen at energies higher than the peak due to the TA branch, and it never appeared to be overdamped at the phase transition. Even in the sample containing 1.4 mol% Li, the scattering from the TO_1 branch remained at energies greater than 30 cm^{-1}.

The apparent absence of a soft mode as noted above, together with the observed gradual increase in the splitting of the B line in Fig. 6, is suggestive of an order-disorder transition of the Li centers, which can couple either to the zone-center TO branch or to a zone-boundary acoustic phonon. The properties of the B line are of importance in deducing the nature of this transition. The line labeled B first appears at a frequency of 75 cm^{-1} at a temperature of about 90 K, which is substantially higher than the temperature of the $T=68$ K transition. As the line softens and splits, its frequency remains in the region of the shoulder which was associated with disorder-induced scattering from the soft TO branch in the previous work on pure $KTaO_3$.[2] This suggests that the low-temperature phase could be a tetragonal-symmetry ferroelectric structure. In that case, the B line would result from the split components with A_1 and E symmetry from the zone-center TO branch. The zone-boundary transverse acoustic branches, however, extend in energy from 45 to ~ 150 cm^{-1}. If the B line is due to scattering from one of these modes, then the low-temperature phase must be antiferrodistortive. If this is the case, other zone-boundary phonons should also become Raman active below 68 K. The poling experiments discussed in Sec. III E are sufficient to distinguish between these two possibilities.

D. Polarization characteristics

The dependence of the Raman spectra on polarization and scattering geometry provides more evidence regarding the nature of the phase transition in $KTaO_3$:Li. In pure $KTaO_3$ the Raman scattering is essentially completely polarized parallel to the incident laser polarization. With the exception of a partial depolarization of the B peak, this is also true above T_c for the $KTaO_3$ sample containing 5.4 mol% Li. The polarization dependence of the Raman spectrum of $KTaO_3$ containing 5.4 mol% Li at 4.2 K is shown in Fig. 7 for two different sample orientations. Due to the depolarization of any light that is not polarized along a cube axis, a detailed study of the polarization characteristics in the low-temperature phase was not possible. With the two experimental geometries indicated in Fig. 7 it is possible to separate the polarized scattering features from the depolarized features. The peaks, B_1 and B_2, that split at the transition from the single peak B have different polarization characteristics; the low-energy peak is composed entirely of depolarized scattering, while the peak at higher energy represents entirely polarized scattering. At 77 K, i.e., well above the transition temperature, the unsplit B peak is observed to have a depolarized component which is approximately one-fourth as in-

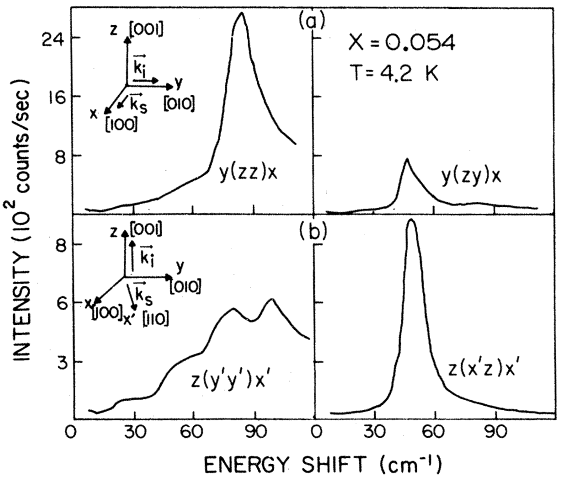

FIG. 7. Polarization dependence at $T=4.2$ K of the Raman spectra of $KTaO_3$ containing 5.4 mol% Li for two different scattering wave vectors. (a) $\vec{k}_{phonon} \parallel \langle 110 \rangle$ axis, (b) $\vec{k}_{phonon} \parallel \langle \sqrt{2}, \sqrt{2}, 1 \rangle$ axis.

tense as the total scattering observed at about 60 cm^{-1}.

The most important feature evident from an examination of Fig. 7 is that the two peaks have not changed energy when the wave vector of the scattered phonon is different either for the two sample orientations or for different domain orientations in either sample orientation. If the peaks B_1 and B_2 resulted from components of the split TO branch in an ordinary tetragonal ferroelectric phase, at least one of the peaks must be an extraordinary phonon which would shift by a substantial fraction of the energy difference between B_1 and B_2. This observation appears to be inconsistent with the behavior expected from a ferroelectric, low-temperature phase in which the anisotropy of the polar lattice with respect to the phonon propagation direction is important. It does, however, appear to be consistent with a transition to an antiferrodistortive, nonpolar, low-temperature phase.

E. Poling experiments

The primary goal of the poling experiment is to produce a monodomain crystal and demonstrate the anisotropy of the extraordinary phonon characteristic of a large polar domain. Figure 8 demonstrates this anisotropy very clearly for the 5.4 mol% Li sample. The data in part (a) were taken after the sample has been cooled to 4.2 K with no field applied. The data in parts (b) and (c) were taken after the sample temperature had been raised above T_c and cooled with a biasing electric field of 1.6 kV/cm. The field was removed after the sample temperature reached 4.2 K and was not reapplied to the sample. The phonons generated in all three parts of Fig. 8 propagate along the cubic phase ⟨110⟩ directions. In part (c), the ⟨110⟩ propagation axis is perpendicular to the polar axis. In this case the ordinary, E-symmetry phonon, polarized perpendicular to the polar axis, and the A_1 phonon, polarized along the polar axis, should be observed. In part (b), the ⟨011⟩ propagation axis has a component along the polar axis, and the extraordinary, or mixed mode, phonon energy should be intermediate between the energies of the ordinary phonon and the pure A_1 phonon. Since the LO phonon energy is 187 cm^{-1}, the LO-TO splitting is considerably larger than the measured anisotropy, and Loudon's[14] simple expression for the energy of the extraordinary phonon,

$$\omega_e^2 = \omega_{\parallel}^2 \sin^2\theta + \omega_{\perp}^2 \cos^2\theta \ , \qquad (1)$$

can be applied. The E symmetry ordinary phonon in Fig. 8 is at $\omega_{\perp} = 43$ cm^{-1}. From Fig. 8(c), the value of $\omega_{\parallel} = 81$ cm^{-1} is obtained for the pure A_1 phonon. Using $\theta = 45°$, Eq. (1) predicts the energy of the extraordinary phonon, $A_1 + E$, in Fig. 8(b) to be 65 cm^{-1}, in excellent agreement with the data.

A study of the polarization characteristics of the peaks in Figs. 8(b) and 8(c) confirms the symmetry of each peak. These symmetries are entirely consistent with a monodomain sample with C_{4v} symmetry and the fourfold (z) axis along the applied electric field. Further evidence of the monodomain character of the poled sample was the observation of birefringence oscillations as the temperature was raised past T_c. The beam was sent through the poled sample parallel to the electrodes with the incident polarization parallel to a ⟨101⟩ axis and the intensity of the light transmitted with perpendicular polarization was monitored, as in the depolarization measurements. The depolarization ratio oscillated as a function of temperature from −1 to +1. This behavior is expected if, rather than depolarizing the beam, the birefringence of a single domain is altering the polarization as the temperature changes. The oscillations as a function of temperature are due to a smooth change in the relative effective path lengths of the components of the beam with polarization parallel and perpendicular to the optical axis. Thus, the change in $\Delta n_T = |n_{\parallel} - n_{\perp}|$ as a function of temperature can be monitored from the frequency of the oscillations which increases as T_c is approached.

This poling experiment was repeated in the sample containing 1.4 mol% lithium. The results are shown in Fig. 9. The effect of poling this sample is to decrease the widths of the peaks so that the sharp E mode can be resolved from the A_1 mode. The larger width of the A_1 phonon compared with the E phonon is suggestive of a very anisotropic damping of the TO

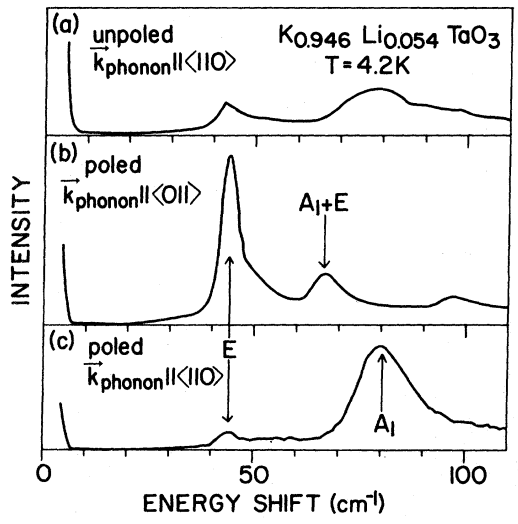

FIG. 8. Raman spectra of $KTaO_3$ containing 5.4 mol% Li at 4.2 K: (a) the unpoled sample, (b) the poled sample with $\theta = 45°$ in Eq. (1), (c) the poled sample with $\theta = 90°$ in Eq. (1). Polarizations included are $Y(ZZ)X$ and $Y(ZY)X$, where X, Y, and Z are pseudocubic axes.

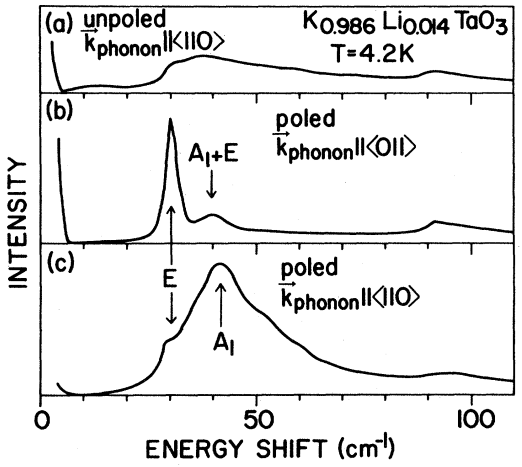

FIG. 9. Raman spectra of $KTaO_3$ containing 1.4 mol% Li at 4.2 K. (a) the unpoled sample, (b) the poled sample with $\theta = 45°$ in Eq. (1), (c) the poled sample with $\theta = 90°$ in Eq. (1). Polarizations are the same as in Fig. 8.

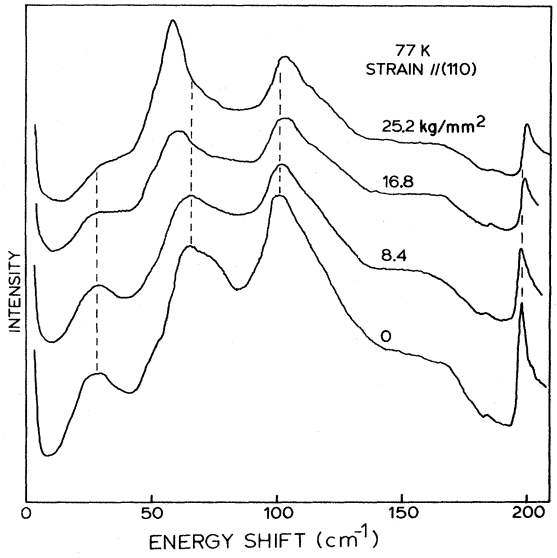

FIG. 10. Raman spectra of $KTaO_3$ containing 5.4 mol% Li as a function of $\langle 110 \rangle$ applied stress at 77 K. Laser light was incident along $\langle 001 \rangle$ and polarized along $\langle 110 \rangle$. No analyzer was used.

branch. A second possible cause of broadening of this peak, however, is its greater sensitivity to lithium concentration, evident in the curves labeled B_1 in Fig. 6. The asymmetric shape of this A_1 mode suggests that inhomogeneities in lithium concentration, or perhaps random strain, may contribute to its breadth.

A complete study of the polarization characteristics and energies of these modes indicates complete agreement with Eq. (1) and behavior identical to that observed in the 5.4 mol% sample, except that the anisotropy at 4 K is $\omega(A_1) - \omega(E) = 13$ cm^{-1}, compared with the value of 38 cm^{-1} for the 5.4 mol% Li sample. Thus, the ferroelectric behavior is clearly observed at a Li concentration as low as $x = 0.014$.

F. Effects of uniaxial stress

Figure 10 illustrates the effects on the Raman spectrum of $KTaO_3$ containing 5.4 mol% Li at 77 K of an increasing uniaxial stress applied along a $\langle 110 \rangle$ axis. As the stress increases, the intensity of the disorder-induced scattering from the TA branch decreases and the intensity of the TO_2 peak near 200 cm^{-1} remains about the same as compared to the intensity of the 2TA peak. The same behavior is observed when the temperature is lowered through T_c. Finally, the scattered intensity in the energy region of the TO_1 shoulder also behaves similarly to the early stages of the temperature-induced transition; a very strong peak, analogous to the B line of Fig. 4, becomes sharper and its intensity increases relative to the 2TA peak as the energy of the peak decreases. Actually, two distinct peaks can be observed when stress is applied. One peak is polarized and the other is depolarized, as they are below the transition temperature in the unpoled samples. Very similar results are obtained with a stress applied along a $\langle 100 \rangle$ axis. The polarizations of the various features with either stress orientation are nearly identical to those observed at zero stress below the 68-K transition temperature. These results indicate that the transition is extremely sensitive to random strains, and caution is required in interpreting the behavior of the material in the temperature region close to the transition.

IV. DISCUSSION

A. Evidence for a ferroelectric phase transition

Recently, the very existence of a low-temperature ferroelectric phase in $KTaO_3$:Li has been in doubt. The depolarization results presented in the previous section indicate that a true phase transition does occur for lithium concentrations greater than 1%. The Raman scattering results in unpoled samples also support this conclusion. The data in Fig. 7 led to an earlier hypothesis that the phase transition involved coupling of off-center lithium ions to the R_{25} zone-boundary acoustic phonon.[15] This model leads to a nonpolar, antiferrodistortive low-temperature phase identical to that of $SrTiO_3$ below 105 K. Preliminary neutron scattering measurements by Axe[16] indicate that the energy of the R_{25} phonon is inconsistent with this hypothesis. Furthermore, the poling experiments described in Sec. III E demonstrate conclusive-

ly that the phonons that are seen as first-order scattering below T_c are polar phonons and, thus, the low-temperature phase is ferroelectric. The fact that poling a sample induces monodomain behavior observed via birefringence is not sufficient to conclude that the low-temperature phase is ferroelectric in unpoled samples. It is conceivable that a random distribution of off-center impurities could induce an antiferrodistortive phase which becomes polar when the dipoles are aligned by the poling electric field or even by internal strains in unpoled samples. Thus, the key evidence is the observation of the anisotropy of the TO phonons in the poled materials.

We now address the question of why the anisotropy is unmistakable in the poled, monodomain samples, yet the data from unpoled samples, as seen in Fig. 7, show no obvious sign of anisotropy. The anisotropy is due to the variation in energy of the extraordinary transverse phonon as it propagates at different angles, θ, with respect to the polar axis. If the domain size is comparable to, or smaller than, the wavelength of the laser light, the wave-vector selection rule is no longer obeyed for the longest wavelength phonons of the domain and scattering will be observed from phonons propagating at all angles θ. If the domain size is small compared to the optical wavelength, the electric field of the exciting laser is nearly uniform over the volume of the domain. In this case, the strongest scattering will be observed from the fundamental modes of vibration of the domain, which have a wavelength twice the domain diameter. Higher order modes will have phase reversals of the ionic displacements and the resulting cancellation effects will rapidly decrease the intensity of the scattering from these modes. If, in addition, the domains are large compared to a lattice spacing, it is clear that the observed scattering will still come from wave vectors very close to $k=0$ in comparison with the zone-boundary wave vector.

These effects can be illustrated using Eq. (1), which gives the frequency of the extraordinary phonon as a function of θ. Since the direction of ionic displacements varies with θ, the scattered intensity from the modes propagating into unit solid angle, Ω, at angles in the range $\theta \rightarrow \theta + d\theta$ to the polar axis is defined as $K(\theta)$. $K(\theta)$ is dependent on the polarization geometry, and may be obtained by decomposing the mixed mode eigenvector into its E and A_1 components and using the usual Raman tensors.[14] The solid angle, $d\Omega = 2\pi \sin\theta d\theta$ subtended by extraordinary phonon wave vectors in the frequency range $\omega_e \rightarrow \omega_e + d\omega_e$ is

$$d\Omega = 2\pi \sin\theta \frac{\partial\theta}{\partial\omega_e} d\omega_e \ ,$$

and the intensity distribution of the scattered light is then

$$I(\omega_e)d\omega_e = 2\pi \sin\theta K(\theta) \frac{\partial\theta}{\partial\omega_e} d\omega_e \ . \qquad (2)$$

Equation (1) can be used to eliminate θ from Eq. (2), and the resulting frequency distribution is

$$I(\omega_e)d\omega_e = \frac{2\pi\omega_e K(\omega_e)d\omega_e}{[(\omega_\parallel^2-\omega_\perp^2)(\omega_\parallel^2-\omega_e^2)]^{1/2}} \ . \qquad (3)$$

This result applies for $\omega_\perp < \omega_e < \omega_\parallel$ and includes only the contribution from the extraordinary phonon.

The intensity factor $K(\omega_e)$ can also be obtained from the polarization-dependent intensities of the pure A_1 phonon and the pure E phonon. Thus,

$$K(\omega_e) = XI(E) + (1-X)I(A_1) \ , \qquad (4)$$

where

$$X = (\omega_\parallel^2-\omega_e^2)/(\omega_\parallel^2-\omega_\perp^2) \ .$$

The square root singularity at $\omega_e = \omega_\parallel$ in Eq. (3) will produce a peak at $\omega_\parallel$ if the polarization geometry is such that the A_1 phonon scattering is allowed, i.e., $K(\omega_\parallel) \neq 0$. This peak will be asymmetric, with a tail extending to a cutoff at $\omega_e = \omega_\perp$ if scattering from the ordinary phonon is allowed, i.e., $K(\omega_\perp) \neq 0$. The scattering from the ordinary phonon, itself, also produces a sharp peak at $\omega_\perp$ for all values of θ.

In the polarized scattering geometry, $I(A_1) \neq 0$, but $I(E) = 0$, and the asymmetric peak at $\omega_\parallel$ will be observable, but the intensity will go to zero before the edge at $\omega_\perp$ is reached. In depolarized scattering, $I(A_1) = 0$, but $I(E) \neq 0$, and an asymmetric peak will exist at $\omega_\perp$ with a tail extending up towards $\omega_\parallel$. All of these features are observed in the data for the 5.4 mol% Li samples in Figs. 4, 7, and 8(a).

Although the large linewidth of the A_1 phonon component obscures some of these shape features in the data for the 1.4 mol% Li sample in Figs. 5 and 9(a), it is clear that these small domain effects can also explain the broad and asymmetric spectra for that sample.

These ideas are also consistent with the results of the experiments with applied stress in which the effects of the stress seemed to be to induce the phase transition, but the application of $\langle 110 \rangle$ stress failed to produce spectra exhibiting polarization selection rules indicative of a single domain with the polar axis perpendicular to the stress. The data can now be explained by the fact that, while the $\langle 110 \rangle$ stress may align domains along the perpendicular $\langle 001 \rangle$ axis, it will *not* necessarily cause all domains to have the same polarity. Therefore, the presence of a fine-grained domain structure in the stressed sample leads to Raman spectra that are similar to the spectra seen at lower temperatures in the unstressed sample.

B. Depolarization and domain size

The discussion of the previous section, shows that, in unpoled samples, the ferroelectric domains have sizes smaller than, or comparable with, an optical

wavelength. Can these domains be small enough to be identified with a single impurity forming a "cluster" as in the polar glass low-temperature phase proposed by Höchli *et al.*?[7] We show in this section that the depolarization behavior in Fig. 3 excludes this possibility. Much larger domains are required to give these depolarization effects.

Julian and Lüty[17] considered a similar problem when they observed optical depolarization effects in the infrared transmission spike of the polycrystalline, birefringent solids KCN and NaCN. They were able to determine an average domain size of 80 μm using the transmission spectrum of wavelengths from 3 to 10 μm and the theoretical development of Raman and Viswanathan,[18] but not using the depolarization information. The geometry of the $K_{1-x}Li_xTaO_3$ problem suggests that the greatest difficulties in the calculation of depolarization effects discussed by Julian and Lüty could be avoided in a simple yet realistic model calculation.

Consider the unpoled ferroelectric as an assembly of evenly stacked, cubic, ferroelectric domains with edges of length, a, and a random distribution of the polar axes along the $\hat{x}$, $\hat{y}$, and $\hat{z}$ directions. The beam propogates along the $\hat{z}$ axis with linear incoming polarization parallel to the $\langle 110 \rangle$ axis. Domains having polar axes parallel to $\hat{z}$ will not affect the polarization of the beam while domains with polar axes parallel to either $\hat{x}$ or $\hat{y}$ will change the relative phases of the two polarization components by equal amounts but with opposite signs. The following assumptions are made to simplify the discussion.

(i) For ease of discussion, divide the total beam transmitted by the crystal into a large number of segments, each of which has passed through a given sequence of domains which is independent of the optical path of the rest of the segments.

(ii) Assume that the domain size is small compared to the sample thickness and beam cross section so that both the number of domains and the number of segments are large. Thus, statistical arguments can be used effectively.

(iii) The effect of any individual domain is to introduce a very small retardation of the phase of one component of the electric field relative to the other. The relative phase shift due to such a domain will be expressed as either $ka(\Delta n)$ or $-ka(\Delta n)$, where k is the magnitude of the optical wave vector, and (Δn) is the difference between the index of refraction parallel and perpendicular to the polar axis. If a is too small, the use of a macroscopic parameter like (Δn) is not rigorous, but the use of that form to describe an effective retardation is still possible.

(iv) The birefringence of an individual domain, (Δn) is the same as the birefringence of the poled material, (Δn_T). The latter can be obtained from the observation that the oscillations in the depolarization ratio of the poled 5.4 mol% lithium sample discussed in Sec. III E imply a change in the phase of

$$\Delta\phi = (\Delta n_T) kl = m(2\pi) \ ,$$

where m is the number of oscillations observed in the temperature range below T_c in which most of the depolarization occurs when the sample has not been poled. Thus,

$$\Delta n = \Delta n_T = m\lambda/l \ , \tag{5}$$

where l is the path length of the beam through the sample. Assumptions (i) and (ii) together would imply that the transformation of the polarized beam above T_c to the unpolarized beam below T_c is due to the dispersion of the magnitudes of the total retardation of the individual segments after transmission through a line of domains. Thus, a polarized exit beam corresponds to a dispersion of zero, while a depolarized beam has a large enough dispersion that the retardation in individual segments ranges nearly evenly between $-\pi$ and π.

Assumption (iii) suggests the application of random walk statistics to the problem of computing the dispersion. Assuming that one-third of the domains will not introduce any retardation, the number of domains that interact with a segment to produce its total relative phase shift will be

$$N = \tfrac{2}{3} l/a \ . \tag{6}$$

The value of N will actually have a statistical variation as well, but the maximum effect of ignoring this variation is to increase the calculated value of a by, at most, 50%. The random walk implies that the average relative phase shift in the beam is zero, but the root-mean-square relative phase shift, the dispersion, is given by $\sqrt{N}$ times the magnitude of the retardation arising from an individual domain. Therefore, to obtain appreciable depolarization, the condition is

$$\pi = \sqrt{N}\,(\Delta n) ka \ .$$

Substituting the expressions in Eqs. (5) and (6) and solving for a gives

$$a = \frac{3l}{8m^2} \ .$$

If the values appropriate to the 5.4 mol% lithium sample, $l = 1$ cm, $m \cong 100$, are inserted, the average domain size is found to be 4000 Å. For the 1.4 mol% Li sample in Fig. 3, the minimum domain size must also be similar to this estimate.

The major error in this calculation is probably the neglect of diffraction, which would violate the condition of independent transmission of the various segments since the beam would not propagate rectilinearly through one line of domains if the wavelength is comparable to, or exceeds, the domain size. This would serve to *reduce* the retardation dispersion from segment to segment and increase the domain size re-

quired to explain the depolarization data.

This domain size calculated from the depolarization measurements is consistent with the requirement, deduced in the previous section, that the domains are smaller than, or comparable to, the 5000-Å optical wavelength. This leads to the conclusion that the domain size is about 5000 Å and is almost certainly in the range from 1000 to 10 000 Å. This is in clear disagreement with the claims[7] that $K_{1-x}Li_xTaO_3$ is not ferroelectric for any $x < 0.24$ and that the interacting Li centers form a polar glass at low temperatures.

C. Order-disorder transition

An additional unusual feature of this class of materials is the order-disorder character of the phase transition, especially when compared to the predominantly soft-mode character of the niobium-induced transition in the same material.[2] The gradual increase of the impurity-induced scattering from the center of the TO_1 branch as the transition temperature is approached from above suggests that a local distortion similar to the one stabilized in the low-temperature phase exists in the vicinity of each Li ion, and that the distortion magnitude, correlation length, or both grow as the transition is approached. Furthermore, the presence of rather sharp impurity-induced scattering features, such as the A line and the TO_2 peak in Fig. 4, indicates the quasistatic nature of the lithium-induced distortion. The linewidths, which are still ~ 10 cm^{-1} at temperatures over 100 K above T_c, define an upper limit for the reorientation frequency of the distortion associated with the lithium ion motion which is smaller than the observed phonon frequencies. These results, then, are in agreement with previous dielectric measurements.[7] They suggest that the lithium impurity is a slowly relaxing, symmetry-breaking defect of the type A1 in the classification scheme of Halperin and Varma,[1] who studied such defects coupled to a soft mode order parameter in the mean-field approximation and the effect of this coupling on phase transitions. They concluded that an order-disorder transition, in association with a strong central peak, occurs at a higher transition temperature than observed in the pure material while the soft mode remains at finite frequency, as we have observed in $K_{1-x}Li_xTaO_3$. The narrow central peak behavior cannot be reliably identified in the Raman spectra, but the other features of the lithium-induced transition are in general agreement with this model. There is no transition in the pure material, however, and the specific approximations used by Halperin and Varma may not be applicable to this material.

A feature of this transition which is still unexplained is the absence of a step in the elastic constants at the transition[6] similar to those observed for the cubic-to-rhombohedral ferroelectric transitions induced by Nb or Na.[10] It is possible that this difference is associated with either the smaller domains or the tetragonal ferroelectric phase induced by lithium.

A final question of interest is whether the transition is of first order or second order in the absence of either a poling field or random strain in the sample. Either the splitting of the E and A_1 phonons or the optical birefringence provides a measurement of the relative magnitude of the order parameter. The data from the unpoled 5.4 mol% Li samples in Fig. 6 imply that any first-order step is a small fraction of the zero-temperature order parameter. In poled 5.4 mol% Li samples, the splitting of E and A_1 is only 6 cm^{-1} for $T_c - T = 10$ K, compared to a total splitting of ~ 40 cm^{-1} at 4.2 K. On the other hand, the hysteresis under reversal of the direction of temperature variation evident in the depolarization data for the 5.4 mol% Li sample in Fig. 3 does suggest a small first-order step at T_c.

ACKNOWLEDGMENTS

We wish to thank John Axe for the very helpful communication of the results of his neutron scattering measurements on $K_{1-x}Li_xTaO_3$ as soon as they had been obtained. The research at Indiana University was supported in part by NSF Grant No. DMR 78-09426. Oak Ridge National Laboratory is operated by the Union Carbide Corporation for the U.S. Department of Energy under Contract No. W-7405-eng-26.

[1] B. I. Halperin and C. M. Varma, Phys. Rev. B 14, 4030 (1976).
[2] R. L. Prater, L. L. Chase, and L. A. Boatner, Phys. Rev. 23, 221 (1981).
[3] Y. Yacoby and A. Linz, Phys. Rev. B 9, 2723 (1974).
[4] Y. Yacoby and S. Yust, Solid State Commun. 15, 715 (1974).
[5] Y. Yacoby, W. B. Holzapfel, and D. Bäuerle, Solid State Commun. 23, 947 (1977).
[6] U. T. Höchli, H. E. Weibel, and L. A. Boatner, Phys. Rev. Lett. 41, 1440 (1978).
[7] U. T. Höchli, H. E. Weibel, and L. A. Boatner, J. Phys. C 12, L563 (1979).
[8] S. Guha and L. L. Chase, Phys. Rev. B 12, 1658 (1975).
[9] L. A. Boatner, A. H. Kayal, and U. T. Höchli, Helv. Phys. Acta 50, 167 (1977).
[10] U. T. Höchli and L. A. Boatner, Phys. Rev. B 20, 266 (1979).

[11]J. D. Axe, J. Harada, and G. Shirane, Phys. Rev. B 1, 1227 (1970).
[12]H. Engstrom, J. B. Bates, and L. A. Boatner, J. Chem. Phys. 73, 1073 (1980).
[13]L. A. Boatner, U. T. Höchli, and H. Weibel, Helv. Phys. Acta 50, 620 (1977).
[14]R. Loudon, Adv. Phys. 13, 423 (1964).
[15]R. L. Prater, L. L. Chase, and L. A. Boatner, Bull. Am. Phys. Soc. 25, 171 (1980).
[16]J. D. Axe (private communication).
[17]M. D. Julian and F. Lüty, Phys. Rev. B 21, 1647 (1980).
[18]C. V. Raman and K. S. Viswanathan, Proc. Indian Acad. Sci. A 41, 37 (1955).